JOURNAL OF GEOPHYSICAL RESEARCH: BIOGEOSCIENCES, VOL. 118, 265–279, doi:10.1002/jgrg.20026, 2013

Modeling burned area in Europe with the Community Land Model

M. Migliavacca,[1] A. Dosio,[1] S. Kloster,[2] D. S. Ward,[3] A. Camia,[1] R. Houborg,[1] T. Houston Durrant,[1] N. Khabarov,[4] A. A. Krasovskii,[4] J. San Miguel-Ayanz,[1] and A. Cescatti[1]

Received 25 September 2012; revised 10 January 2013; accepted 12 January 2013; published 18 March 2013.

[1] In this study, we present simulations of a burned area at a European scale for the period 1990–2009 conducted with the Community Land Model (CLM). By using statistics on fire counts and mean fire suppression time from the European Fire Database, we refined the parameterization of the functions describing human ignition/suppression, and we modified the description of biomass availability for fires. The results obtained with the modified model show an improvement of the description of the spatial and interannual variability of the burned area: the model bias is reduced by 45%, and the explained variance is increased by about 9% compared to the original parameterization of the model. The observed relationships between burned area, climate (temperature and precipitation), and aboveground biomass are also reproduced more accurately by the modified model. This is particularly relevant for the applicability of the model to simulate future fire regimes under different climate conditions. However, results showed an overestimation of the burned area for some European countries (e.g., Spain and France) and an underestimation in years with an extreme fire season in Mediterranean countries. Our results highlight the need for refining the parameterization of human ignition/suppression and fuel availability for regional application of fire models implemented in land surface models.

Citation: Migliavacca, M., A. Dosio, S. Kloster, D. S. Ward, A. Camia, R. Houborg, T. Houston Durrant, N. Khabarov, A. A. Krasovskii, J. San Miguel-Ayanz, and A. Cescatti (2013), Modeling burned area in Europe with the Community Land Model, *J. Geophys. Res. Biogeosci.*, *118*, 265–279, doi:10.1002/jgrg.20026.

1. Introduction

[2] Fires are one of the main disturbances affecting terrestrial ecosystems and have a profound impact on global climate, air quality (through emissions of greenhouse gases, black carbon, aerosols, and their precursors), surface albedo, and vegetation structure and functioning [e.g., *Bowman et al*., 2005; *Randerson et al*., 2006; *Arneth et al*., 2001]. Climate variability has the potential to significantly impact fire regimes (i.e., spatial patterns, frequency, and intensity) and burned area [e.g., *Flannigan et al*., 2000; *Meehl et al*., 2007). Historical evidence suggests that fire regimes were strongly controlled by climate prior to human settlement [e.g., *Swetnam and Betancourt*, 1998; *Pechony and Shindell*, 2010; *Brown et al*., 2005; *Heyerdahl et al*., 2002; *Heyerdahl et al*., 2008). These analyses demonstrate, for example, a strong correlation between years of widespread fire and low precipitation, that lead to a regional depletion of soil moisture and, ultimately, to a low moisture content in foliage and in fine and dead surface fuels [*Swetnam and Betancourt*, 1998].

[3] Besides climate, fire activity is also affected by human factors. On one hand, humans influence fire patterns by igniting fires (intentionally or accidentally); on the other hand, humans actively suppress both anthropogenic and natural fires. Moreover, *Bowman et al*. [2005] showed that ecosystem management (e.g., clearing forests, promoting grazing, dispersing plants) may either increase or decrease background levels of natural fire activity. Many studies conducted at local [e.g., *Guyette et al*., 2002; *Martell et al*., 1989], regional [e.g., *Venevsky et al*., 2002; *Costa et al*., 2011], and global [e.g., *Pechony and Shindell*, 2009] scales apply an empirical relationship between population density and anthropogenic ignition sources and human suppression. These studies highlighted that the probability of fire occurrence and the chances of fire suppression increase as population density increases.

[4] In Europe, fires are a major threat to human lives and property, with disastrous impacts on ecosystems [e.g., Rego et al., 2010]. Fire is an intrinsic key disturbance in Mediterranean ecosystems, where the number of fires has increased dramatically during recent decades, mostly due to changes in

[1]European Commission—Joint Research Centre (JRC), Institute for Environment and Sustainability, Ispra, Varese, Italy.
[2]Land in the Earth System, Max Planck Institute for Meteorology, Hamburg, Germany.
[3]Department of Earth and Atmospheric Science, Cornell University, Ithaca, New York, USA.
[4]Ecosystems Services and Management Program, International Institute for Applied Systems Analysis (IIASA), Laxenburg, Austria.

Corresponding author: M. Migliavacca, European Commission—Joint Research Centre (JRC), Institute for Environment and Sustainability, Via E. Fermi, 2749, I-21027 Ispra (VA), Italy. (mirco.migliavacca@jrc.ec.europa.eu)

2169-8953/13/10.1002/jgrg.20026

land use [*Pausas*, 2004; *Pausas et al*., 2008] and to socio-economic drivers, but also to the improvement in statistical reporting of fires [*San-Miguel-Ayanz and Camia*, 2009]. On average, about 0.5×10^6 ha are burned every year in the five southern European Union member states (Portugal, Spain, Greece, Italy, and France) [*European Commission*, 2009]. Moreover, the impact of events of extreme fires is increasing. For instance, in 2003, Portugal experienced an exceptionally large forest burned area, which contributed to turn the land use, land-use change and forestry (LULUCF) sector from a net sink into a carbon source of 7076 Gg CO_2 [FCCC, 2006].

[5] In Southern Europe, over the next 100 years, climate change is expected to result in summer temperature increases of up to 4–5°C and decreases in rainfall during summer of up to 50% [*Christensen et al*., 2007]. Because summer drought and burned area are strongly linked in this area [*Pausas*, 2004; *Camia and Amatulli*, 2009; *Carvalho et al*., 2010], the projected increase of temperature and drought intensity might lead to an increase in fire potential, which, in turn, will very likely become an even more serious threat to Mediterranean forests and human well-being, especially in rural areas [e.g., *Lindner et al*., 2010]. As an example, for Portugal, *Carvalho et al*. [2010] showed that dramatic increases in fire occurrence and burned area of respectively 279% and 478% are predicted for 2071–2100 in comparison with the 1980–1990 period. On the other hand, climate change will probably decrease net primary productivity of forests in Southern and continental Europe [*Alcamo et al*., 2007], and consequently, a reduction of total fuel availability is expected. To evaluate the joint effect of increased fire risk and reduced availability of fuel, there is the need to use land surface models.

[6] In this context, understanding and modeling the interactions between climate, fires, and vegetation is essential [e.g., *Flannigan et al*., 2000]. A few models have been developed to simulate fire occurrence and burned area predictively in land surface models. *Thonicke et al*. [2001] related burned area and fire season length by means of an empirically derived relationship. *Arora and Boer* [2005] used a process-based approach by parameterizing the burned area as a function of fire spread rate. *Pechony and Shindell* [2009] developed a global-scale fire parameterization for fire favorable environmental conditions based on water vapor pressure deficits. Recently, *Thonicke et al*. [2010] and *Prentice et al*. [2010] presented a fire model within the Lund-Potsdam-Jena dynamic global vegetation model. Finally, building on previous models [*Arora and Boer*, 2005; *Thonicke et al*., 2001], a new fire model was implemented by *Kloster et al*. [2010] within the framework of the Community Land Model (CLM).

[7] Regional and global fire models developed in the last decade, embedded in the state-of-the-art land surface models, incorporate the explicit description of both natural and anthropogenic sources of ignition, as well as anthropogenic fire suppression, obtaining a reasonable representation of fire occurrence at global and regional scales [e.g., *Kloster et al*., 2010; *Pechony and Shindell*, 2009; *Li et al*., 2012a; *Thonicke et al*., 2010]. The anthropogenic ignition/suppression is modeled as a function of population density [e.g., *Kloster et al*., 2010; *Pechony and Shindell*, 2009]. For instance, in the work of *Kloster et al*. [2010], human influences on fire regimes are modeled assuming that in highly populated areas, fires are detected earlier and suppressed more effectively than in sparsely populated areas.

[8] Given the complexity of fires as a process, and the spatial and temporal variability of the anthropogenic causes, parameters of global-scale models are often uncertain, and data are needed to refine the equations and parameterization governing, in particular, human ignition/suppression. This is even more important when land surface models are applied at regional to continental scales, as global parameterization might lead to misleading results. Therefore, to improve present and future assessment of the impacts of fire in Europe, there is the need to validate and, if necessary, to refine the description of fire patterns at a continental scale as simulated by land surface models that are designed and calibrated for global-scale applications.

[9] In this study, we used CLM3.5 [e.g., *Stöckli et al*., 2008; *Thornton et al*., 2007; *Thornton et al*., 2009; *Randerson et al*., 2009; *Lawrence et al*., 2011] with the fire routine implemented by *Kloster et al*. [2010], which follows the approach described by *Arora and Boer* [2005] (hereafter referred to as CLM-AB).

[10] The objectives of the analysis are the following: (i) to develop a modified version of CLM-AB with a calibrated parameterization of human/ignition suppression and fuel availability for its application in Europe (hereafter, we refer to the modified model as CLM-AB MOD), (ii) to evaluate the fire routines CLM-AB and CLM-AB MOD for regional estimates of burned area against independent data sets, and (iii) to evaluate if CLM-AB MOD is able to mimic the observed relationships between temperature, precipitation, and aboveground biomass in Europe and, therefore, to understand if the proposed model can be a useful tool for forecasting burned area under a climate change scenario.

[11] In section 2, we describe the model structure, the data used in this study and the simulation protocol, the procedure for model calibration, and the statistical analysis conducted. In section 3, we present the results of model refinement, with focus on the evaluation of the spatial and interannual variability of the burned area, and the relationship between burned area and climate in Europe. In section 4, we discuss first the model improvements, second the limitations of the current modeling approach and the future research directions to overcome the limitations highlighted, and, finally, the relationship between burned area, climate, and vegetation.

2. Methods

2.1. Model Overview

[12] All simulations conducted in this study were performed with a modified version of the CLM version 3.5 [e.g., *Stöckli et al*., 2008] extended with a carbon-nitrogen biogeochemical model [*Thornton et al*., 2007; *Thornton et al*., 2009; *Randerson et al*., 2009]. Most of the updates of the model are described by *Lawrence et al*. [2011].

[13] A comprehensive evaluation of the gross primary productivity and CO_2 land-atmosphere exchanges simulated by CLM and other state-of-the-art terrestrial biosphere models was recently performed by comparing modeled and observed carbon fluxes at several eddy covariance flux tower sites distributed across North America [*Schaefer et al*., 2012; *Keenan et al*., 2012].

[14] The prognostic treatment of fires is based on the fire algorithm developed by *Arora and Boer* [2005], modified and implemented within CLM by *Kloster et al*. [2010].

[15] Currently, within the CLM community, four different fire models are available although not all yet released within the official versions of the model [*Thonicke et al*., 2001; *Kloster et al*., 2010; *Li et al*., 2012a; *Li et al*., 2012b]. The models differ in particular in the prediction of fire ignition occurrence. In the work of *Thonicke et al*. [2001], annual burned area depends on fire season length and fire occurrence probability. Fire occurrence probability is not related to anthropogenic causes but depends on fuel availability and soil moisture. *Kloster et al*. [2010] introduced, first, the anthropogenic ignition probability and fire suppression, and then the description of deforestation fires. Furthermore, *Li et al*. [2012a], building on *Kloster et al*. [2010], proposed a new fire routine with a different description of fire occurrence and a new global parameterization estimated by constraining model parameters with MODIS Active Fire Count products. Finally, *Li et al*. [2012b] introduced (i) a new parameterization of peat fires, (ii) an alternative scheme for deforestation fires, and (iii) a different representation of anthropogenic impacts on fires, including the Gross Domestic Product as an additional driver to account for the effects of socioeconomic variables on fire occurrence.

[16] CLM-AB was already successfully implemented and evaluated to simulate fires for the 20th and 21st century at a global scale [*Kloster et al*., 2010; *Kloster et al*., 2012].

[17] Here, the fire algorithm is briefly described. Further information can be found in *Kloster et al*. [2010].

[18] The total probability of fire occurrence (P) is estimated as the product of three separate probabilities: the probability related to biomass availability (P_b), the probability conditioned on the moisture (P_m), and the probability of ignition (P_i). P_b takes into account the availability of biomass for burning (i.e., total fuel load) and is defined as

$$P_b = \max\left[0, \min\left(1, \frac{F - F_l}{F_u - F_l}\right)\right] \tag{1}$$

where F is the aboveground biomass (sum of leaf, stem, litter, and coarse woody debris pools), and F_l and F_u are constants set to 200 gC/m^2 and to 1000 gC/m^2, respectively.

[19] P_m is expressed as

$$P_m = 1 - \tanh\left(\frac{1.75m}{m_e}\right)^2 \tag{2}$$

where m is the plant available volumetric water content in the top 5 cm of the soil, m is used as a surrogate for fuel moisture content [*Thonicke et al*., 2001], and m_e is the moisture of extinction, defined here as 0.35, independent of fuel type [*Kloster et al*., 2010].

[20] One of the main improvements of *Kloster et al*. [2010] is the introduction of an ignition probability, P_i, variable in space and time, in contrast to the original formulation by *Arora and Boer* [2005]. Ignition can be either natural (lightning) or human induced.

[21] Natural ignition probability (P_l) is controlled by lightning and is a function of cloud to ground lightning frequency LF (flashes/km^2/month), which is linearly scaled between essentially no flashes (LFlow = 0.02 flashes/km^2/month) and the maximum observed values (LFup=0.70 flashes/km^2/month).

$$P_l = \beta/(\beta + \exp(1.5 - 6\beta)) \tag{3}$$

where $\beta = max[0, min(1, (LF - LFlow)/(LFup - LFlow))]$.

[22] The human ignition probability (P_h) is described by using the relationship developed by *Venevsky et al*. [2002], further modified by *Kloster et al*. [2010], which relates fire occurrence to population density (ρ) in terms of interactions of humans with natural ecosystems:

$$P_h = \min\left(1, \frac{\rho \cdot 6.8 \cdot \rho^{-0.57}}{\rho_{up} \cdot 6.8 \cdot \rho_{up}^{-0.57}}\right) \tag{4}$$

where ρ_{up} is set as 300 inhabitants/km^2.

[23] Fire suppression probability (F_s) also depends on the population density. According to *Kloster et al*. [2010], fire suppression is more likely to take place in densely populated areas, where typically high property values are at risk [*Theobald and Romme*, 2007; *Stocks et al*., 2003] and more resources and infrastructures are available for suppression. Fire suppression is parameterized similarly to *Pechony and Shindell* [2009]:

$$F_s = 1.0 - \left(a + e^{b \cdot \rho}\right) \tag{5}$$

where $a = 0.10$ and $b = 0.025$. Equation (5) assumes that fire suppression increases as ρ increases, and in more densely populated areas, 90% of the fires are suppressed.

[24] Finally, total ignition probability is calculated as

$$P_i = [(P_l + (1 - P_l) \cdot P_h] \cdot (1 - F_s) \tag{6}$$

[25] Figure 1 illustrates P_h, F_s, and P_i as a function of ρ. P_i shows a peak of around 20 inhabitants/km^2, which is in agreement with the analysis performed by *Barbosa et al*. [1999] for Africa.

[26] The parameterization of human ignition and fire suppression functions (equations (4), (5), and (6)) in the work of *Kloster et al*. [2010] is derived for application at a global scale.

[27] The model then computes the burned area at each time step according to *Arora and Boer* [2005] as described by *Kloster et al*. [2010]. The fire is assumed to spread from the ignition point as an ellipse. The shape of the ellipse depends on fire spread rates in upwind and downwind directions as well as the length-to-breath ratio [*Arora and Boer*, 2005; *Kloster et al*., 2010]. Fire spread rate is a function of wind speed and soil moisture.

[28] Although not relevant for Europe for contemporary periods, CLM-AB also represents deforestation fires by allowing for a variable fraction of deforestation carbon to be combusted, with the fraction depending on fuel conditions during the year of land clearing [*Kloster et al*., 2010].

2.2. Data for Model Calibration and Evaluation

[29] The model predictions of burned area are evaluated against the statistics reported in the European Fire Database [*European Commission*, 2011; *European Commission*, 2009] and the Global Fires Emissions Database Version 3 (GFED) [*Giglio et al*., 2010; *van der Werf et al*., 2010].

[30] The European Fire Database contains information on fires compiled by European Union member states and other European countries within the framework of the European

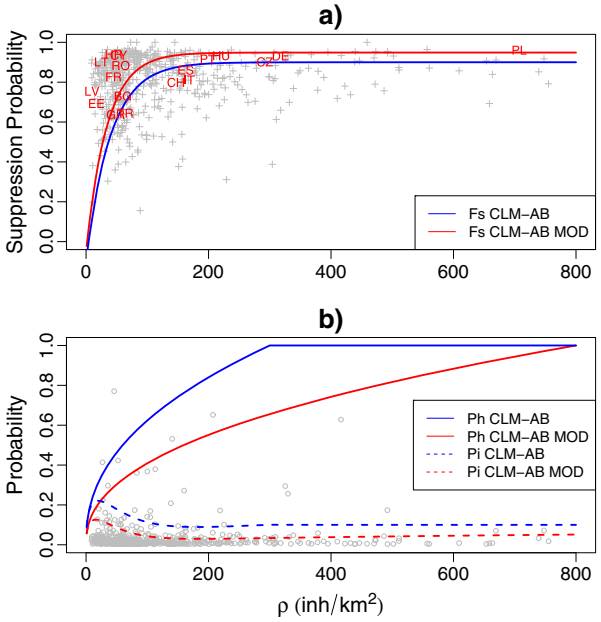

Figure 1. (a) Fire suppression probability (Fs) as function of population density (ρ). The grey crosses represent the suppression probability computed as in equation (5) and derived from the European Forest Database of the European Forest Fires Information System. The codes reported represent the suppression probability averaged by country. The mean (ρ) for each country corresponds to the mean (ρ) of the NUTS3 for which fires are reported. The country codes follow the ISO two-character system: Bulgaria (BG), Croatia (HR), Cyprus (CY), Czech Republic (CZ), Estonia (EE), Finland (FI), France (FR), Germany (DE), Greece (GR), Hungary (HU), Italy (IT), Latvia (LV), Lithuania (LI), Poland (PL), Portugal (PT), Romania (RO), Slovakia (SK), Slovenia (SL), Spain (ES), Sweden (SE), and Switzerland (CH). (b) Human ignition (Ph) and unsuppressed ignition probability (Pi) as a function of the population density. The gray circles represent the total ignition probability (Pi) in a day derived from the European Fires Database of the European Forest Fires Information System. In both panels, red lines represent the functions as in those in the work of *Kloster et al*. [2010], while blue lines represent the calibrated functions.

Forest Fire Information System (EFFIS). EFFIS has been established by the Joint Research Centre and Directorate General for Environment of the European Commission to support fire management in Europe, with the contributions of the national forest fire services in the countries. At the time of writing, the database contains fire data from 22 of the countries who participate in the EFFIS network (Bulgaria, Croatia, Cyprus, Czech Republic, Estonia, Finland, France, Germany, Greece, Hungary, Italy, Latvia, Lithuania, Poland, Portugal, Romania, Slovakia, Slovenia, Spain, Sweden, Switzerland, and Turkey) with length of records variable across countries. From the available data, we used monthly records of burned area, mean fire suppression time (i.e., fire duration from the first alert to the complete suppression), and fire counts. Data are available at the level of NUTS3 regions (Nomenclature of Units for Territorial Statistics, EUROSTAT, version 2006), which correspond to local administrative units of variable area (ranging from 43.4 km^2—Luton—to 25,388 km^2—Goteborg), based on the existing national administrative subdivisions (i.e., districts for Germany, province for Italy and Spain, groups of municipalities for Portugal, etc.).

[31] The GFED is a global data set containing monthly estimates of burned area [*Giglio et al*., 2010] and emissions from biomass burning [*van der Werf et al*., 2010] since July 1996 at 0.5 degree spatial resolution. The burned area reported in GFED is a satellite product based on Moderate Resolution Imaging Spectroradiometer (MODIS) fire counts, surface reflectances, and land-cover characteristics [*Giglio et al*., 2010]. The GFED data set represents the most comprehensive attempt to date to derive burned area, as well as pyrogenic fluxes, from remote sensing data and provides a suitable source of information for validating and improving fire models [e.g., *Prentice et al*., 2010].

2.3. Model Calibration and Development

[32] The statistics and data about fire counts and suppression time reported in EFFIS are used to calibrate the parameters of the suppression (equation (5)) and ignition (equation (6)) functions.

[33] As a first step, the parameters of the suppression function (equation (5)) are calibrated.

[34] For each NUTS3, the probability of suppression, F_s, is computed by using the formulation suggested by *Arora and Boer* [2005]:

$$F_s = \frac{1}{1+\tau} \tag{7}$$

where τ represents the mean fire suppression time [day] reported in EFFIS for each NUTS3. By using F_s estimated from EFFIS (equation (7)) and the population density data, the parameters a and b of equation (5) are calibrated. The EUROSTAT statistics for population density at the NUTS3 level are used because they are already aggregated over NUTS3 territorial units and, therefore, consistent with the fires statistics.

[35] As a second step, the ignition probability function (P, equation (6)) is calibrated.

[36] The total daily ignition probability for each NUTS3 is computed as the ratio between the fires counted for each NUTS3, reported in EFFIS, and the length of the record in days. Then, using the total ignition probability estimated and the population density for each NUTS3, we estimated the parameter ρ_{up} (defined in equation (4)), that controls P_h in equation (6). In this second step, the parameters of F_s in equation (6) are fixed to the values estimated in the first step.

[37] Parameters were estimated by using a generalized nonlinear least squares optimization function [*R Development Core Team*, 2011].

[38] Furthermore, the description of P_b (equation (1)) was modified by removing the stem biomass from the total aboveground biomass used in the original formulation, which was developed for application on boreal forests [*Kloster et al*., 2010; *Arora and Boer*, 2005]. Therefore, in CLM-AB MOD, we used the coarse woody debris, litter, and biomass of the crown layer (i.e., leaves) as model drivers. This modification was included because, in temperate and Mediterranean ecosystems, the biomass of the surface and crown layer is considered the best descriptor of the fuel load, rather than the total

aboveground biomass [*Thonicke et al*., 2001; *Pyne et al*., 1996]. The parameters for the computation of (P_b) were set according to the calibrated values reported by *Li et al*. [2012a] as $F_l = 155$ gC m^{-2} and $F_u = 1050$ gC m^{-2}.

2.4. Forcing Data and Simulation Protocol

[39] We performed two different runs for the period 1991–2009, the first with CLM-AB and the second with CLM-AB MOD. Runs were conducted at a spatial resolution of 0.9 × 1.2 degree (Gaussian grid). Model runs were performed at half-hourly time steps.

[40] As meteorological forcing, the ERA-Interim reanalysis obtained from the European Centre for Medium-Range Weather Forecasts (ECMWF) was used [*Dee et al*., 2011]. We used 6 hourly data of air temperature, wind speed, specific humidity, and atmospheric pressure, and 3 hourly total shortwave incoming radiation and precipitation.

[41] Lightning frequency was obtained from the NASA Lightning Imaging Sensor/Optical Transient Detector product (LIS/OTD), which reports total flash rates (cloud-to-ground and intracloud flashes). LIS/OTD is a daily product. Here it is aggregated as a monthly climatology variable and is therefore assumed constant from year to year. Although this assumption can potentially be seen as a limitation for the description of the interannual variability of P_l (equation (3)), it can be considered robust because the percentage of fires ignited by lightnings in Europe is low (about 5% according to *Rego et al*. [2010]) compared to the fires ignited by humans.

[42] Population density data for model runs were taken from the HYDE data set [*Klein Goldewijk*, 2001] and regridded to match the model resolution applied in this study.

[43] The initial conditions for the model runs are simulated as described in the CLM user guide documentation (http://www.cesm.ucar.edu/models/cesm1.0/clm/models/lnd/clm/doc/UsersGuide/x9300.html). To reach the steady state of the carbon pools simulated, we first run the model for 600 simulation years from arbitrary initial conditions using the "accelerated decomposition spin-up" mode and the model forcing released with CESM. Then, a stationary climate forcing data set was constructed by repeating 1979-1994 ERA-Interim detrended data, similarly to *Prentice et al*. [2010]. The spin-up proceeded by using the CLM normal mode and the stationary climate data until the equilibrium of carbon pools were reached.

2.5. Statistical Analysis

[44] To evaluate the accuracy of the model results, the mean absolute error (MAE), the determination coefficient (r^2, i.e., the total observational variance explained by the model), the Pearson's correlation coefficient (r), and the Reduced Major Axis linear regression coefficients between observed (EFFIS and GFED) and modeled (CLM-AB and CLM-AB MOD) burned area were computed [*Janssen and Heuberger*, 1995]. RMA regression was preferred to ordinary least squares (OLS) linear regression analysis because one of the assumptions of OLS (i.e., error on y $>>$ error on x) is not met. In fact, the observations (i.e., GFED) are partly modeled, and therefore, the error might be comparable to that of the simulation.

[45] The cross-correlation between observed and modeled monthly burned area at a country scale was also computed. This analysis was conducted to identify the time lag that maximizes the correlation between observed and modeled time series and, therefore, to verify if the summer peak of burned area occurs in the same month in observations and models. Positive (negative) time lags indicate that the model leads (follow) the observations, i.e., the peak of modeled burned area occurs earlier (later) than the peak in the observations. Ideally, time lags should be 0 (i.e., peak of burned area modeled and observed occurs at the same month).

[46] We also computed the performance statistics (r and MAE) between deseasonalized simulated and observed monthly burned area at a country level. Deseasonalization (i.e., the process of removing the seasonal variations from a time series) is useful for exploring the trend and any remaining irregular component derived from monthly burned area. This analysis was conducted to assess the capability of the model to explain the fast (i.e., monthly) and slow (seasonal) variations in observed burned area, and to evaluate the performance of the model at different time scales [e.g., *Mahecha et al*., 2010]. The deseasonalization was performed by using a time series decomposition method based on the running average [*Kendall and Stuart*, 1983] and implemented in R [*R Development Core Team*, 2011].

[47] For each country, the interquartile distance (IQD) of the annual burned area time series was computed. IQD is computed as the difference between the 75th and the 25th percentiles of the observed and simulated annual burned area for each country ($IQD = Q_{0.75} - Q_{0.25}$). The linear regression analysis between observed and modeled IQD was used to evaluate the performance of models to describe the interannual variability of the burned area.

[48] To understand how the model reproduces the spatial variability of the mean burned area, the linear regression between observed and modeled mean burned area for each country for the simulation period was computed.

[49] Finally, the distribution of mean observed and modeled burned areas for mean monthly temperature, precipitation, and aboveground biomass classes were computed. The resulting distributions allowed us to quantify the accuracy of CLM-AB and CLM-AB MOD to describe the relationship between climate, productivity, and burned area [e.g., *Prentice et al*., 2010].

3. Results

3.1. Calibration of Model Parameters

[50] Figure 1 shows P_h (equation (4)), F_s (equation (5)), and P_i (equation (6)) as functions of population density (ρ). Blue lines represent the original model (CLM-AB), and red lines represent the optimized parameterization implemented in the modified model (CLM-AB MOD). The parameters obtained after the calibration for the computation of P_i (equation (6)) with CLM-AB MOD at a European scale are as follows: ρ_{up}=800 inhabitants/km^2 (i.e., parameter of the human ignition probability function, equation (4)), $a = 0.0514$, and $b = 0.0292$ (i.e., parameters of the fire suppression probability, equation (5)).

[51] The MAE between original and calibrated F_s decreased from 0.16 to 0.13 after calibration. The improvement is larger for P_i, with MAE decreasing from 0.12 to 0.06 after calibration.

[52] The new parameterization leads to a lower P_i (Figure 1b) by reducing P_h and increasing F_s. As a result, a lower P_i is expected for the same population density, compared to the original parameterization. The peak of the calibrated P_i occurs at a lower population density (about 16 inhabitants/km^2) compared to CLM-AB (about 20 inhabitants/km^2).

[53] Regarding suppression (equation (5)), the new parameterization assumes that, in more densely populated areas ($\rho >$ 200 inhabitants/km^2), 95% of the fires are suppressed with an increase of about 5% compared to the original parameterization.

[54] Maps of the relative differences of P_i simulated with CLM-AB MOD and CLM-AB are shown in Figure 2a, and relative differences of P_b are shown in Figure 2b. Finally, the mean of the monthly total fire occurrence probability (P) simulated with CLM-AB and CLM-AB MOD is shown in Figures 2c and 2d, respectively.

[55] The calibrated parameters lead to a relative decrease of P_i ranging from –30% in Northern Europe to –70% in Central Europe (Figure 2a). The modified P_b is also generally reduced by up to 90% in the United Kingdom, Ireland, and Northern Scandinavia.

[56] The relative contribution of P_i to the reduction of the total fire occurrence probability is in general higher than P_b although the spatial patterns are different. P_i reduction plays an important role in Western, Central, and Eastern Europe, while the reduction of P_b plays an important role in Northern Scandinavia, in the Southern Iberian Peninsula, in Northern France, Northern Germany, and in the United Kingdom. As both P_i and P_b simulated with the modified model are lower than the original ones, the total occurrence probability (P) simulated with CLM-AB MOD (Figure 2d) is lower than that simulated with CLM-AB (Figure 2c). Differences are observed everywhere in Europe with a large reduction in the Mediterranean basins and in the Balkan regions. A reduction of P_i is also observed in Central Europe and in Northern Europe.

3.2. Evaluation of Spatial and Interannual Variability of Simulated Burned Area

[57] Time series of simulated and observed monthly burned areas are shown in Figure 3 for the countries that are most affected by fires in Europe [*European Commission*, 2011]. Evidently, modeled burned area systematically overestimates the observations, in particular in France and in Spain, for both versions of the model. However, CLM-AB MOD generally improves the predictions of monthly and annual burned area at a country scale; the improvement of the results is particularly pronounced in Southern Europe (Greece, Italy, Portugal, and Spain). The tendency to overestimate burned area with CLM-AB MOD is evident also in Figure 4, which depicts the mean seasonal cycle of burned area averaged over the period 1997–2009.

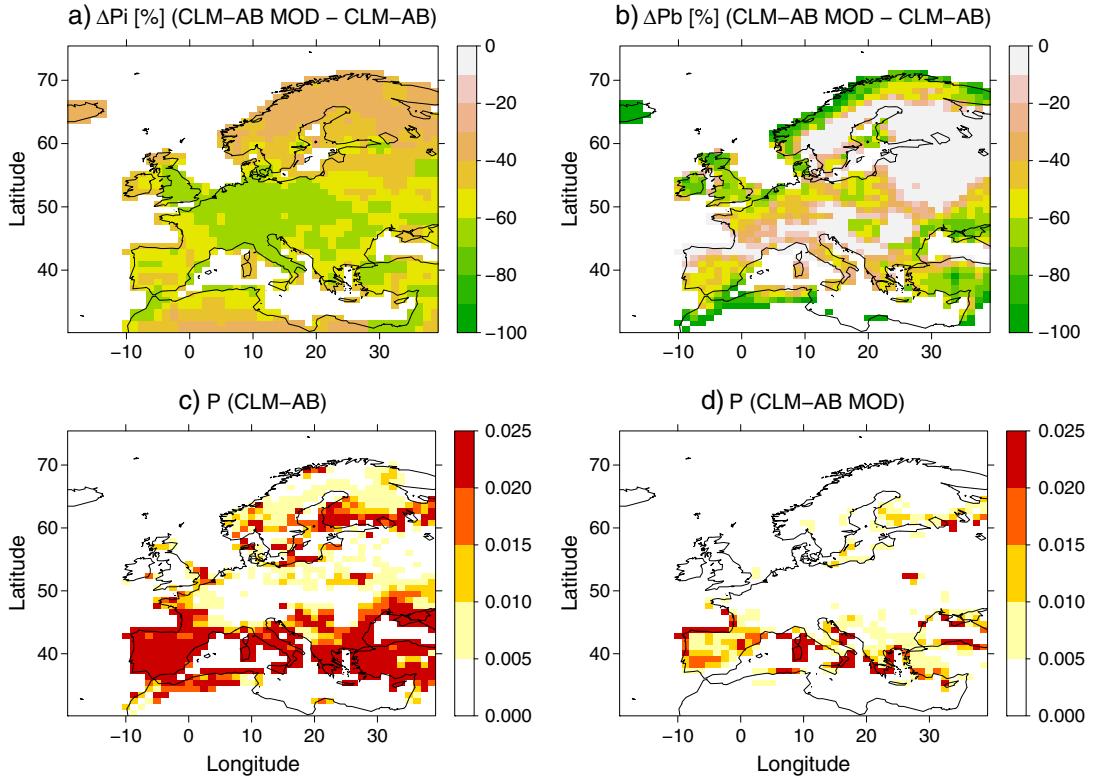

Figure 2. (a) Map of the percentage differences of the ignition probability (Pi, equation (6)) as computed with the original parameterization (CLM-AB) and the modified model (CLM-AB MOD). (b) Map of the percentage differences of the probability related to biomass availability (Pb, equation (1)) as computed with the original parameterization (CLM-AB) and the modified model (CLM-AB MOD). (c) Map of the probability of fires occurrence (P) for CLM-AB. (d) Map of the probability of fires occurrence (P) for CLM-AB MOD.

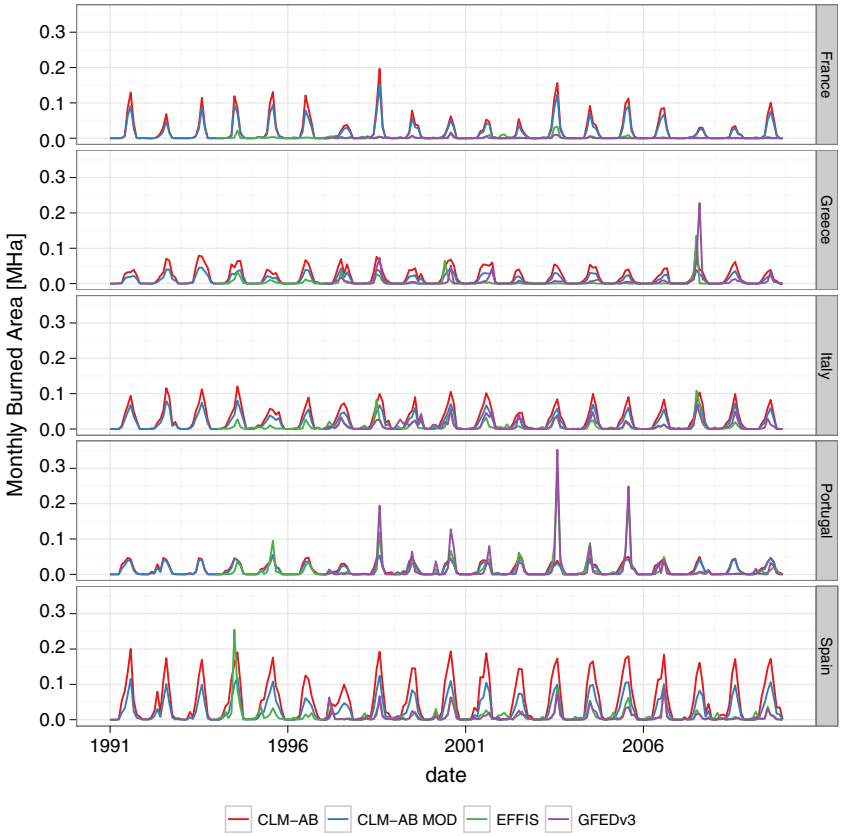

Figure 3. Time series of monthly burned area for the five European countries that mostly contribute to the annual amount of burned area in Europe (Spain, Greece, Italy, Portugal, and France). Different lines represent the burned area simulated by CLM-AB (red) and CLM-AB MOD (blue), and the burned area reported in the European Forest Fires Information System (EFFIS, green) and in the Global Fires Emission Database (GFEDv3, purple).

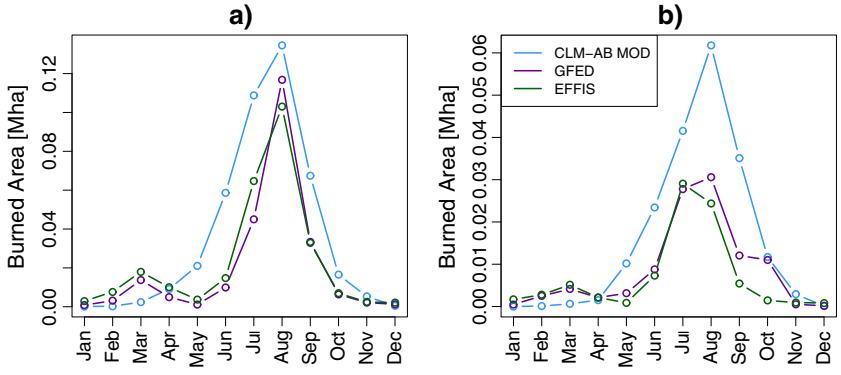

Figure 4. Time series of mean seasonal cycle of monthly burned area, averaged over the period 1997–2009, for (a) the Iberian Peninsula and for (b) Italy. Different lines represent the burned area simulated by CLM-AB MOD (blue) and reported in the European Forest Fires Information System (EFFIS, green) and in the Global Fires Emission Database (GFED, purple).

[58] Figures 3 and 4 show that monthly estimates of GFED are in agreement with EFFIS, although differences exist during certain years in Italy and Greece. These differences may partly be explained by omission errors in GFED due to undetected small fires [*Kaiser et al.*, 2012], particularly in rural areas.

[59] Model performance statistics (r, MAE) between simulated and observed monthly burned area, for countries with more than 4 years of data reported in EFFIS, are shown in Table 1. The statistics of the deseasonalized time series are shown in Table 2.

[60] The new parameterization leads to an improvement of the correlation between observed and modeled data and a large reduction of MAE (Table 1). For example, for Spain, MAE is reduced from 0.0422 Mha/month to 0.0195 Mha/

Table 1. Statistics of the Correlation Between Monthly Observed (GFED and EFFIS) and Modeled (CLM-AB and CLM-AB MOD) Burned Area[a]

Country	CLM-AB						CLM-AB MOD					
	EFFIS			GFED			EFFIS			GFED		
	r	MAE	Lag	*r*	MAE	Lag	*r*	MAE	Lag	*r*	MAE	Lag
Bulgaria	–	–	–	0.57	0.0062	0.00	– –	–	–	0.58	0.0045	0.00
Czech Republic	–	–	–	0.18 ns	0.0001	0.00	– –	–	–	0.17 ns	0.0001	0.00
Germany	0.14 ns	0.0024	0.58	0.02 ns	0.0010	–1.00	0.14 ns	0.0022	0.58	0.02 ns	0.0007	–1.00
Spain	0.52	0.0422	0.00	0.64	0.0422	0.00	0.55	0.0197	0.00	0.66	0.0195	0.00
Finland	–	–	–	0.02 ns	0.0025	1.00	–	–	–	0.02 ns	0.0013	0.75
France	0.55	0.0157	0.00	0.53	0.0160	0.00	0.57	0.0120	0.00	0.53	0.0122	0.00
Greece	0.45	0.0150	0.00	0.41	0.0130	0.00	0.44	0.0085	0.00	0.43	0.0074	0.00
Croatia	0.45	0.0039	0.00	0.71	0.0025	0.00	0.46	0.0036	0.00	0.74	0.0019	0.00
Hungary	–	–	–	0.13	0.0019	1.00	–	–	–	0.14	0.0008	1.17
Italy	0.63	0.0186	0.00	0.77	0.0161	0.00	0.65	0.0110	0.00	0.78	0.0092	0.00
Poland	0.10 ns	0.0027	0.67	0.30	0.0022	0.00	0.09 ns	0.0014	0.67	0.32	0.0009	0.00
Portugal	0.55	0.0109	0.00	0.49	0.0135	0.00	0.56	0.0098	0.00	0.51	0.0120	0.00
Romania	–	–	–	0.40	0.0066	1.00	–	0.0014	–	0.35	0.0060	1.00
Sweden	0.62	0.0007	0.00	0.27	0.0008	0.00	0.64	0.0003	0.00	0.26	0.0005	0.00
Slovakia	–	–	–	0.27	4.8e–5	–0.08	–	–	–	0.29	3.9e–5	0.00

[a]*r* is the Pearson's correlation coefficient ($p < 0.01$). MAE is the Mean Absolute Error. Lag represents the time lag (month) that maximize the cross-correlation coefficients between observed and modeled burned area. ns indicates nonsignificant correlations. Data are reported for the European countries with long time series (> 7 years) in EFFIS.

Table 2. Statistics of the Correlation Between Deseasonalized Monthly Observed (GFED and EFFIS) and Modeled (CLM-AB and CLM-AB MOD) Burned Area[a]

Country	CLM-AB				CLM-AB MOD			
	EFFIS		GFED		EFFIS		GFED	
	r	MAE	*r*	MAE	*r*	MAE	*r*	MAE
Bulgaria	–	–	0.36	0.0056	–	–	0.41	0.0045
Czech Republic	–	–	0.03 ns	0.0003	–	–	0.04 ns	0.0002
Germany	0.13 ns	0.0025	–0.02 ns	0.0012	0.14 ns	0.0024	–0.02 ns	0.0008
Spain	0.28	0.0126	0.37	0.0116	0.37	0.0087	0.44	0.0076
Finland	–	–	0.06 ns	0.0027	–	–	0.06 ns	0.0018
France	0.38	0.0096	0.34	0.0101	0.41	0.0072	0.33	0.0077
Greece	0.28	0.0069	0.21	0.0075	0.28	0.0054	0.23	0.0068
Croatia	0.42	0.0033	0.63	0.0017	0.43	0.0031	0.69	0.0014
Hungary	–	–	0.01 ns	0.0019	–	–	–0.02 ns	0.0009
Italy	0.38	0.0066	0.49	0.0057	0.37	0.0053	0.50	0.0049
Poland	0.17 ns	0.0031	0.24	0.0029	0.16	0.0015	0.23	0.0013
Portugal	0.20	0.0116	0.24	0.0154	0.17	0.0115	0.24	0.0152
Romania	–	0.0047	0.11 ns	0.0076		0.0035	0.05 ns	0.0071
Sweden	0.54	0.0007	0.31	0.0008	0.59	0.0004	0.30	0.0005
Slovakia	–	–	0.09 ns	8.5e–5	–	–	0.11 ns	0.0001

[a]*r* is the Pearson's correlation coefficient ($p < 0.01$). MAE is the Mean Absolute Error. Lag represents the time lag (month) that maximizes the cross-correlation coefficients between observed and modeled burned area. ns indicates non-significant correlations. Data are reported for the European countries with long time series (>7 years) in EFFIS.

month; for Italy, Portugal, France, and Greece, a reduction of MAE ranging from about 0.0069 Mha/month to 0.0037 Mha/month is observed.

[61] For the majority of the countries, the cross-correlation analysis does not identify a lag between observed and modeled burned area (Table 1). This means that the month at which the peak of the burned area occurs is reproduced well by both versions of the model, with a few exceptions in Central and Eastern Europe: for Germany, we find that the peak of modeled burned area occurs 1 month later than the observed one, whereas the models simulates a peak of burned area 1 month earlier than observations for Hungary, Romania, and Poland.

[62] Table 2 shows that the deseasonalized monthly burned area statistics also improve slightly by using the modified model, even though the overall performance statistics are poorer than those obtained with the monthly time series (Table 1). When the seasonal cycle is removed, the capability of the model to describe the remaining monthly variability of burned area is poor overall: statistically significant *r* ranging from 0.20 to 0.63 for CLM-AB, and from 0.16 to 0.69 for CLM-AB MOD (Table 2). Although the modified model explains the mean seasonal cycle well, the monthly variability of burned area is difficult to predict due to the stochasticity of the phenomena. For instance, monthly burned area is poorly described in early spring in some Mediterranean countries (Spain, Portugal, and Italy), where the recurrent peak in burned area observed is not accurately modeled (Figure 4). Moreover, for years with an

extreme fire season in summer (e.g., Greece and Italy in 2007, Portugal in 2003 and 2005, and Spain in 1994), both models fail to reproduce the peak in observed burned area.

[63] Figure 5 shows the scatterplot between observed and modeled annual burned area. Single points represent 1 year for one country, while different colors represent different geographic areas: Mediterranean countries (France, Greece, Italy, Portugal, and Spain) are shown in orange, Northern European countries (Finland and Sweden) in blue, and Central and Eastern European countries (the remaining countries) in red. The improvement of the simulation of annual burned area using CLM-AB MOD compared to CLM-AB is evident in Figures 5a–5d. By using CLM-AB MOD, we observe a similar variance explained by the models (r^2) and a reduction of the MAE of the mean annual burned area of about –47% for EFFIS and –43% for GFED. The scatterplot between GFED and EFFIS annual burned area (Figure 5e) shows good agreement between the two observational data sets ($r = 0.84$, slope = 0.77, MAE = 0.0219 Mha/yr). CLM-AB MOD explained the variability of the annual burned area well in Central and Northern Europe (red and blue dots in Figure 5), while for Mediterranean countries, the year-to-year variability is not completely represented by the model. For Mediterranean countries, the models simulate, on one hand, an overall larger burned area and, on the other hand, a lower year-to-year variability.

[64] Figure 6a is a scatterplot of modeled and observed mean annual burned area for each country, where the burned area has been averaged over the years in which data are available in the EFFIS data set. The spatial variability of burned area at a country level reported in the EFFIS is reasonably represented by CLM-AB MOD ($r^2 = 0.88$, slope = 0.54, MAE = 0.0429 Mha/yr) with a reduction of the overestimation of the mean burned area for each country of about 50% compared to CLM-AB (MAE decreases from 0.0909 Mha/yr to 0.0429 Mha/yr) (Figure 6a).

[65] Figures 6b and 6c show the relationship between modeled and observed IQD for GFED and EFFIS data. Because IQD is an indicator of the interannual variability of burned area at a country scale, the results show that year-to-year variations of the burned area at a country level is better explained by CLM-AB MOD (increase of r^2, Figures 6b and 6c) with a reduction of the underestimation of IQD (slope of linear regression increases from 0.36 to 0.76 for EFFIS and from 0.67 to 1.1 for GFED).

3.3. Relationship Between Burned Area, Climate, and Aboveground Biomass

[66] Figure 7 shows the distribution of modeled and observed monthly burned area in classes of mean monthly temperature (Figure 7a), precipitation (Figure 7b), and aboveground biomass (Figure 7c).

[67] The distributions of observed burned area reported in GFED have a pronounced unimodal relationship, for both precipitation and temperature, as already reported in other studies in the tropics [*Prentice et al*., 2010], and are in agreement with the conceptual model proposed by *Murphy et al*. [2011] that relates fires frequency with environmental drivers such as aridity and vegetation productivity. CLM-AB, CLM-AB MOD and GFED show the same general patterns of the relationship between burned area and climate (i.e., unimodal distributions), with a maximum of burned area around the precipitation rate of 12 mm/month, and around 24°C for temperature. Mean burned area values are higher for CLM-AB while CLM-AB MOD and GFED are in good agreement. The bias of CLM-AB is mainly due to the overestimation of burned area in Central and Eastern Europe as well as in Spain.

[68] CLM-AB MOD slightly underestimates the burned area for values of precipitation ranging from 70 to 170 mm/month, and in months with mean temperatures higher than 30°C. This suggests that fire regimes in CLM-AB MOD are more limited by high temperatures (and therefore by biomass availability) than reported by GFED.

[69] In addition, the distribution of observed burned area in classes of aboveground biomass is unimodal, with a maximum at about 500 gC/m^2. For low values of aboveground biomass, the burned area is lower due to fuel limitations. The simulations conducted with CLM-AB MOD also improve the description of the observed relationship between burned area and aboveground biomass.

4. Discussion

4.1. Model Improvements

[70] In this study, we presented a modified version of the fires routine implemented in the CLM modeling framework (CLM-AB MOD), for application at a European scale.

[71] By using fire counts and mean suppression time statistics from the European Fire Database (contained in EFFIS), we refined the parameterization of the functions describing human ignition/suppression, and we modified the description of fuel availability. With the proposed parameterization, a reduction of ignition probability ranging from –30% in Northern Europe to –70% in Central Europe is expected for the same population density (Figure 2). Moreover, the probability of suppression decreases by about 5% compared to the original parameterization. In addition, the modified formulation of the biomass probability (P_b) leads to a reduction of the total fire occurrence probability, in particular in Northern Scandinavia, in the United Kingdom, and in the Southern Iberian Peninsula.

[72] Our results suggest that by calibrating the parameters of the equations describing human ignition/suppression (equations (4), (5), and (6)) and refining the description of biomass probability (equation (1)), the simulation of the burned area is substantially improved. By using the statistics reported in EFFIS, we were able to tune the global parameterization of CLM-AB, thereby providing a more robust description of the spatial and temporal pattern of the burned area in Europe. This confirms that the approach used for the simulation of human-induced ignition and suppression, based on *Pechony and Shindell* [2009] and *Venevsky et al*. [2002], is robust for its application over Europe. Nevertheless, regional-specific parameterizations [*Pechony and Shindell*, 2009] and a refined description of biomass probability [e.g., *Pyne et al*., 1996] need to be developed.

[73] The increasing availability of data sets containing fire counts represent a unique opportunity to improve the spatial description of ignition sources as already shown in global modeling studies [e.g., *Li et al*., 2012a; *Li et al*., 2012b]. On the contrary, the availability of statistics (e.g., fire duration) for fire suppression is limited. In this context, efforts to collect such statistics in a consistent and systematic way (e.g., EFFIS) is crucial as the gathered information is valuable for further

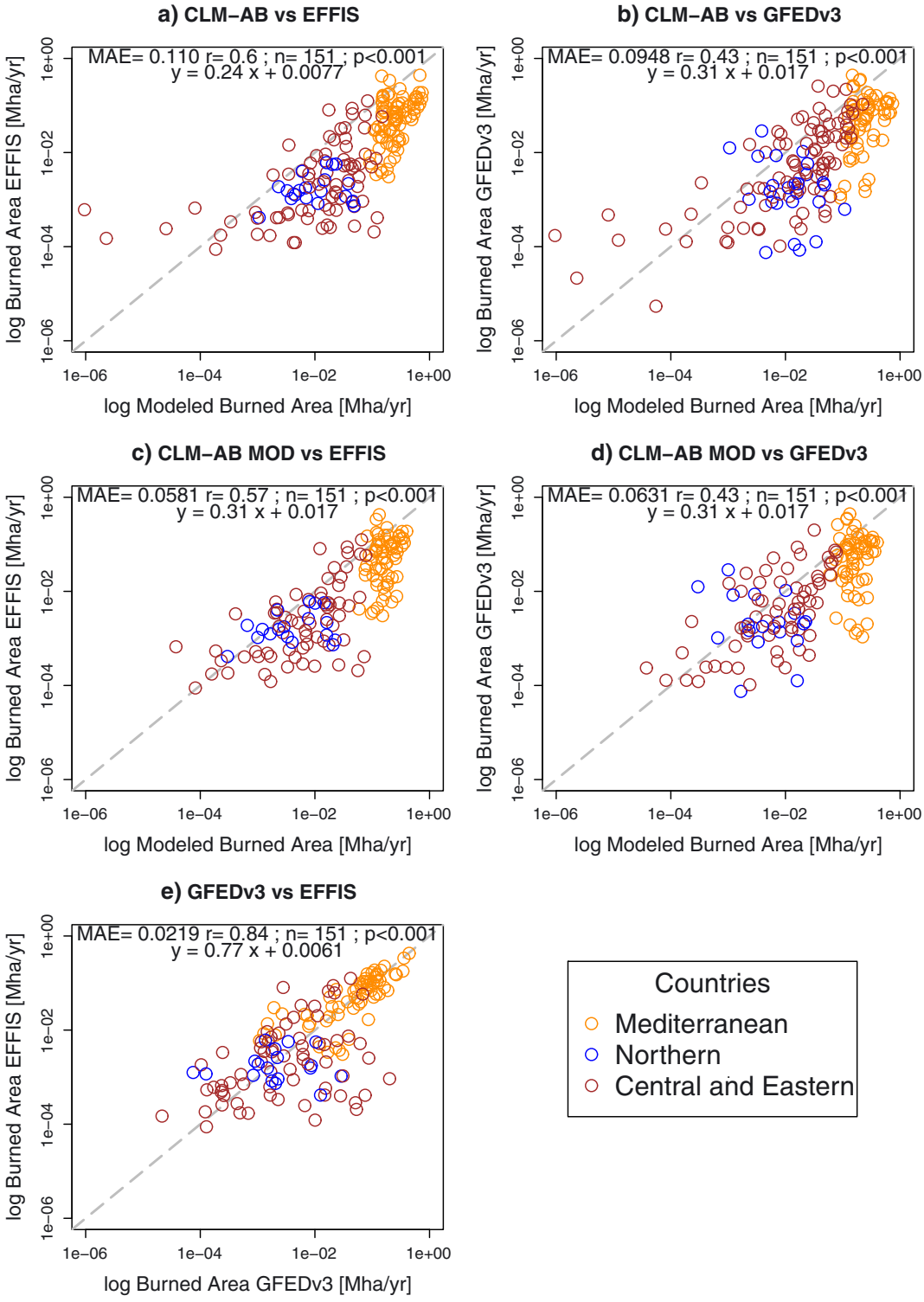

Figure 5. (a, b, c, d) Scatterplot of observed versus modeled annual burned area for the all European countries. (e) Scatterplot of burned area reported in the European Forest Fires Information System (EFFIS) and in the Global Forest Emissions Database (GFED). CLM-AB is the forest fires routine developed by *Kloster et al*. [2012]. CLM-AB MOD represents the forest fires model calibrated in this study. Mean Absolute Error (MAE), Pearson's correlation coefficient, and the coefficients of the Reduced Major Axis regression analysis are also reported. The dashed gray line represents the 1:1 line. Different colors represent the climatic area of each country (Mediterranean: orange, temperate areas: red, boreal countries: blue).

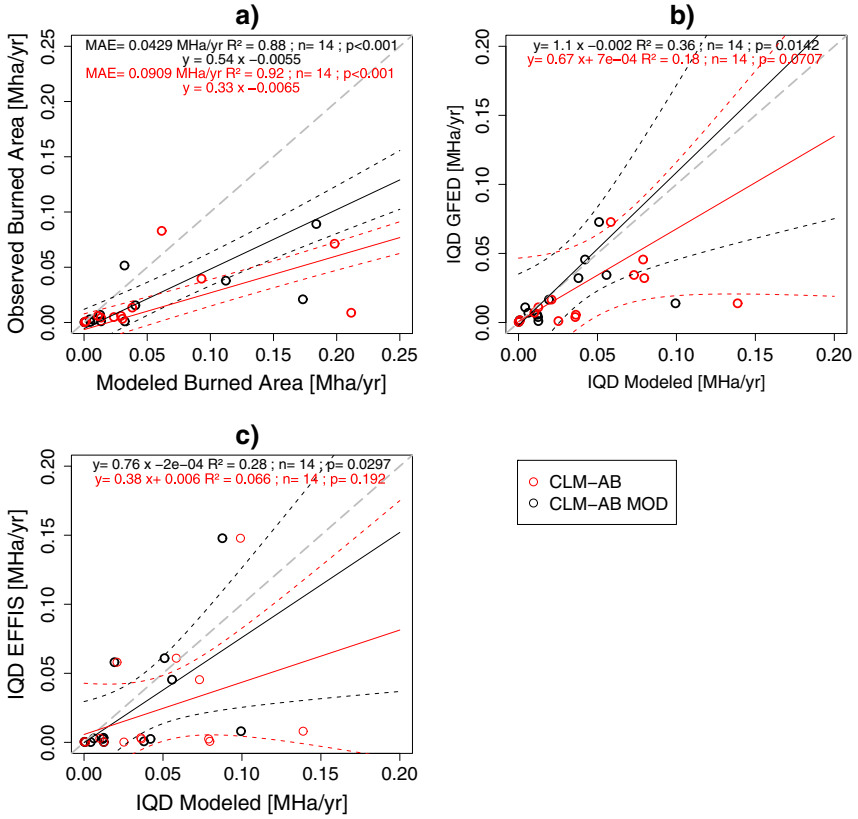

Figure 6. (a) Scatterplot of observed versus modeled mean annual burned area (BA) for each European country reported in the EFFIS database. (b) Scatterplot of the interquartile distance (IQD) of modeled and observed (GFED) burned area for each country. IQD is computed as the difference between the burned area at the 0.75 and 0.25 percentiles. (c) Scatterplot of IQD of modeled and observed (EFFIS) burned area for each country. Red circles represent data obtained with CLM-AB while black circles represent data obtained with CLM-AB MOD. Solid red and black lines represent the linear regression between modeled (CLM-AB and CLM AB MOD, respectively) and observed data. 95% confidence intervals are also reported (dashed red and black lines). Mean Absolute Error (MAE), determination coefficient (r^2), and coefficients of linear regression analysis are also reported.

refining and calibrating fire routines in land surface models and for better constraining model parameters as shown in this study. Our results demonstrate that regional and continental scale data sets containing statistics on fires provide important information to improve the understanding of the human influence on fires and the parameterization of ignition/suppression functions in process-based fire models.

[74] However, a unique parameterization, solely based on the population density, of the process-based fire models might be insufficient considering the variability in the causes of ignition and the differences of resources for fire prevention and suppression. As a further improvement, it should be considered that an adequate representation of anthropogenic influences requires not only information on population densities but also comprehensive global socioeconomic data on sources of anthropogenic ignitions, fire suppression policies and resources, and fire prevention efforts [e.g., *Chuvieco et al*., 2008; *De Wilde and Chapin*, 2006]. Fire management policies and their effectiveness depend on cultural, economical, and other factors. This information is needed for estimating anthropogenic influence both in the past and in the future. At present, however, such information, including information on pastoral activity, is unavailable or highly uncertain at the global scale [*Chuvieco et al*., 2008] and sparsely available at the regional scale.

4.2. Limitations of the current modeling approach

[75] Our results emphasize a reduction of the bias in modeled burned area using CLM-AB MOD and, to a lesser extent, an improvement of the explained variance both at monthly and annual time scales.

[76] Despite the improvement, CLM-AB MOD still shows some limitations in modeling burned area. Specifically, the model (1) overestimates the burned area, although the bias is substantially reduced compared to the original model; (2) systematically underestimates burned area in years with severe fire seasons (extremely high burned area); and (3) does not properly describe the burned area in late summer-autumn in Mediterranean countries.

[77] 1. One of the reasons for the overestimation of the burned area in Europe might be related to the fire spread rate simulated by CLM-AB, which does not account for the spatial fragmentation of the fuel. In fact, land fragmentation by agricultural fields may break the fuel continuity, therefore acting as an important factor hindering fire spread, with the

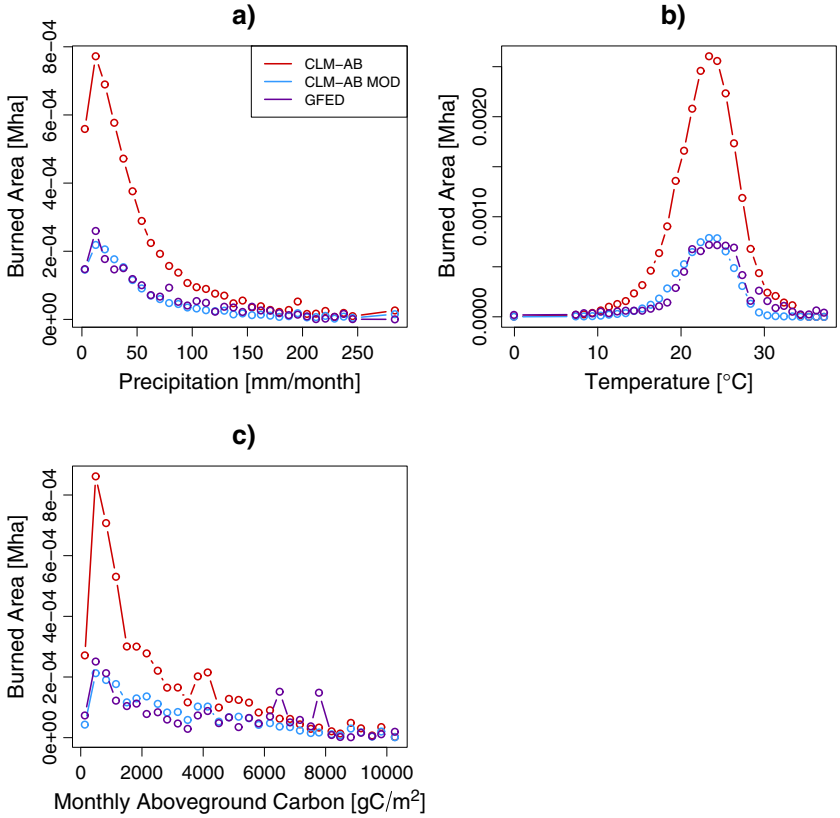

Figure 7. Burned area in bins of mean monthly (a) temperature, (b) precipitation, and (c) aboveground biomass according to CLM-AB (red lines), CLM-AB MOD (blue lines), and GFED (purple lines).

consequent reduction of burned area [*Lloret et al*., 2002; *Loepfe et al*., 2010; *Loepfe et al*., 2012].

[78] 2. CLM-AB and CLM-AB MOD cannot reproduce the extreme events observed, such as the 2003 fires season in Portugal and the extremely high burned area observed in Greece and Italy during the summer of 2007 (Figure 3). The poor description of extreme burned area or large fire events is one of the most diffuse problems of empirical or process-based fire models [e.g., *Thonicke et al*., 2010], which tend to miss large burned areas in the most extreme years. A better process understanding and description of the fire environment and the management context that lead to extreme fire events and large burned areas are important to quantify the impacts of fires on society, ecosystems, and on the emissions of greenhouse gases from lands [e.g., *Bacciu et al*., 2011; *Barbosa et al*., 2009]. Considering that large fires have a significant impact on natural, social, and economic systems in Europe, future research should focus on accurate modeling of the burned area during extreme fire seasons.

[79] The underestimation of burned area observed in severe fire seasons might be related to the model structure, rather than to the absence of extreme weather events into the meteorological forcing. In fact, *Simmons et al*. [2010] showed that ERA-Interim reanalysis reproduces the interannual variability of climate in Europe and, for this reason, is often used to analyze the impacts of extreme events on carbon and water cycles [e.g., *Mueller and Seneviratne*, 2012]. Important limitations for the simulation of large fires might be related, first, to an incomplete description of the fuel-weather interactions and, second, to a poor description of the temporal dynamics of fire suppression, which is most often assumed constant in time in fire models.

[80] Regarding the first cause, severe meteorological conditions, such as extreme temperatures and prolonged drought periods, are the main drivers for major fire events [e.g., *Camia and Amatulli*, 2009]. With these conditions, when fuel is available, fires escaping initial attack might easily develop into major fire events, and for this reason, prevention strategies in Europe are often focused on avoiding or limiting these unmanageable situations through appropriate fuel management [*San-Miguel-Ayanz et al*., 2013]. The current description of fuel and moisture probability implemented in CLM-AB (equations (1) and (2)) might not be sufficiently flexible to describe properly the nonlinear response of fires to weather in these conditions (fuel availability and severe drought conditions) and fuel/weather interactions [e.g., *Slocum et al*., 2010].

[81] Regarding the second cause, an efficient firefighting organization can usually cope with individual ignitions. However, when multiple ignitions occur or during severe fire seasons, the availability of resources can become limited, and suppression resources allocated to one fire are not available for additional fires [*Preisler and Westerling*, 2007]. Therefore, the larger the number of simultaneous ignitions or the longer the duration of multiple fires, the lower the overall efficiency of the suppression [e.g., *Podour and Martell*, 2007; *Husari and McKelvey*, 1996]. To the best of our knowledge, the dependence of suppression on the

number of ignited fires and on the length of fires is not explicitly incorporated in the state-of-the-art fire routines implemented in land surface models and can be considered one of the causes of the poor description of large fire events.

[82] 3. The monthly model-observation mismatch in autumn and in March in the Mediterranean region is plausibly related to the timing of the silvo-pastoral management, pasture burning, and, therefore, to human activities. The relationship between wildfires and pastoralism in Mediterranean areas is well known: *Rego et al*. [2010] reported that in Portugal, fires related to pastoral activities occur in midsummer, midautumn, and at the end of winter/beginning of spring, with year-to-year differences in the fire season related to the meteorological conditions and food availability for cattle. Although autumn burned area in the Mediterranean area comprises only 7% of the total burned area, and fire related to pastoral activity is about 11% of the total wildfires [*Rego et al*., 2010], the explicit description of the effects of silvo-pastoral management should be included in process-based fire models for proper assessment of the seasonal variability of burned area. For the time being, including the fine description of the timing of ignition sources related to traditional land use practices might introduce large uncertainties given the scarce availability of spatially explicit information on pastoral management. Future efforts should address this limitation.

4.3. Modeling the Relationship Between Burned Area, Climate, and Vegetation

[83] Process-based fire modeling is the key toward the development of scenarios that relate fire occurrence, burned area, and climate change [e.g., *Kloster et al*., 2012; *Prentice et al*., 2010; *Murphy et al*., 2011]. Therefore, it is crucial to assess the predictive ability of the model related to simulating the relationship between burned area and climate.

[84] Recently, *Murphy et al*. [2011] and *Krawchuk and Moritz* [2011] showed a conceptual nonlinear relationship between fire frequency, biomass, and aridity. The conceptual model assumes a limited burned area in very dry, unproductive environments (very warm temperatures and very low precipitations), where the fires are typically limited by biomass availability, while in wet and productive ecosystems, fires are limited by high fuel moisture. As a consequence, the fire activity tends to be more prominent at intermediate levels of aridity (warm temperatures and low precipitation) and productivity. Our results show that this conceptual model is also valid in Europe, as demonstrated by the analysis with GFED, and well reproduced by CLM-AB MOD.

[85] The unimodal distribution of burned area in classes of temperature and precipitation (Figure 7) is due to fuel limitation in dry conditions and moisture limitation under wet conditions [e.g., *Prentice et al*., 2010; *van der Werf et al*., 2008]. On one hand, high precipitation rates lead to a decrease in fire probability; on the other hand, low precipitation rates limit biomass accumulation, which decreases fire probability and, eventually, burned area.

[86] The modified model reduces the bias of the burned area simulated at a specific temperature, precipitation, and aboveground vegetation biomass, compared to the original parameterization (Figure 7). Moreover, the sensitivity of the burned area simulated with CLM-AB MOD to these environmental drivers is comparable with observations, given that a variation of one driver (e.g., +1°C of temperature) leads to a variation of burned area similar to the ones reported in GFED (blue and purple lines in Figure 7).

[87] These results demonstrate that the description of the relationship between burned area and the main environmental drivers, for a specific application at the continental scale, can be improved by introducing few modifications in the model parameterization: first, refining the description of the patterns of human ignition/suppression and, second, modifying the description of biomass probability.

[88] This is particularly promising as *Murphy et al*. [2011] emphasize that a key research challenge is to evaluate if process models developed for global applications are able to realistically reproduce the main characteristics of fire regimes and the sensitivity to climate variations at different spatial scales. Refinements to the regional parameterization of fire models could have important implications for improving the analysis of the sensitivity of fire occurrence probability and burned area to climate change.

5. Conclusions

[89] In this study, we presented simulations of burned area at the European scale for the period 1991–2009 conducted with a modified fire model implemented in the CLM.

[90] On the basis of our results, we demonstrate that when applied at the regional scale, the use of the parameterization developed for the global-scale application is limiting, in particular considering the variability of the causes of ignition and the differences of resources for fire prevention and suppression.

[91] Given the availability of spatially explicit maps of fire counts derived from satellite data, such as the GFED database, and, when available, statistical records on fire events, we suggest that development of regional-specific parameterizations for human-induced ignition and suppression is feasible, and here, we propose a specific parameterization for use over Europe.

[92] The description of the fire probability related to biomass availability (i.e., description of fuel) also needs to be accurately defined and refined at the regional scale.

[93] Some limitations of the current modeling approach were identified, particularly in relation to the simulations of extreme events.

[94] The ability of the proposed model to mimic the observed relationship between burned area, climate (temperature and precipitation), and vegetation productivity (aboveground biomass) is promising and is relevant for the application of the CLM fire routine to simulate the sensitivity of fire occurrence probability and burned area to climate change in Europe.

[95] **Acknowledgments.** This research was undertaken as part of the Integrated Projects called MEDIATION (Methodology for Effective Decision-making on Impacts and Adaptation) and IMPACT2C (Quantifying projected impacts under 2C warming). These projects are funded by the European Commission, FP7, under contract numbers 244012 and 282746, respectively. M.M. acknowledges the European Centre for Medium-Range Weather Forecasts (ECMWF) Special Project and the Super Computing Applications and Innovation department of CINECA Consortium for providing the support to run the Community Land Model. The authors acknowledge Louis Giglio and Guido van der Werf for providing the GFED database and Natalie M. Mahowald, Olivier Morgan, and Francesco Fava for their contributions and fruitful discussions.

References

Alcamo, J., J. M. Moreno, B. Novky, M. Bindi, R. Corobov, R. J. N. Devoy, C. Giannakopoulos, E. Martin, J. E. Olesen, and A. Shvidenko (2007), Europe, in Climate change 2007: Impacts, Adaptation and Vulnerability - Contribution of Working Group II to the Fourth Assessment Report of the Intergovernmental Panel on Climate Change, edited by M.L. Parry, O.F. Canziani, J.P. Palutikof, P.J. van der Linden and C.E. Hanson, pp. 541–580, Cambridge University Press, Cambridge.

Arneth, A., et al. (2001), Terrestrial biogeochemical feedbacks in the climate system, *Nature Geosciences*, *3*(8), 525–532.

Arora, V. K., and G. J. Boer (2005), Fire as an interactive component of dynamic vegetation models, *Journal of Geophysical Research*, *110*(G2), doi:10.1029/2005JG000042.

Bacciu, V. M., M. Salis, G. Pellizzaro, B. Arca, P. Duce, and D. Spano (2011), Carbon loss and greenhouse gas emission from extreme fire events occurred in Sardinia, Italy, *American Geophysical Union, Fall Meeting 2011*, abstract no. B23C-0447.

Barbosa, P. M., A. Camia, J. Kucera, G. Libertá, I. Palumbo, J. San Miguel–Ayanz, and G. Smuck (2009), Chapter 8 Assessment of Forest Fire Impacts and Emissions in the European Union Based on the European Forest Fire Information System, in Developments in Environmental Science, edited by A. Bytnerowicz, M. Arbaugh, A. Riebau, and C. Andersen, pp. 197–208, Elsevier, Amsterdam.

Barbosa, P. M., D. Stroppiana, and J. M. Grégoire (1999), An assessment of vegetation fire in Africa (1981-91): Burned areas, burned biomass, and atmospheric emissions, *Global Biogeochemical Cycles*, *13*(4), 933–950.

Bowman, D. M. J. S., et al. (2005), Fire cycles in North American interior grasslands and their relation to prairie drought, *Proceedings of the National Academy of Sciences (USA)*, *50*(5), 133–140.

Brown, K. J., J. S. Clark, E. C. Grimm, J. J. Donovan, P. G. Mueller, B. C. Hansen, and I. Stefanova (2005), Fire cycles in North American interior grasslands and their relation to prairie drought, *Proceedings of the National Academy of Sciences (USA)*, *50*(5), 133–140.

Camia, A., and Amatulli, G. (2009), Weather Factors and Fire Danger in the Mediterraneans, in *Earth Observation of Wildland Fires in Mediterranean Ecosystems*, edited by: E. Chuvieco, pp. 71–82, Springer-Verlag, Berlin.

Carvalho, A., M. Flannigan, K. Logan, L. Gowman, A. Miranda, and C. Borrego (2010), The impact of spatial resolution on area burned and fire occurrence projections in Portugal under climate change, *Climatic Change*, *98*(1), 177–197.

Christensen, J. H., et al. (2007), Regional climate projections, in Climate change 2007: The physical science basis - Contribution of Working Group I to the Fourth Assessment Report of the Intergovernmental Panel on Climate Change, edited by S. Solomon, D. Qin, M. Manning, Z. Chen, M. Marquis, K.B. Averyt, M. Tignor, and H.L. Miller, pp. 847–940, Cambridge University Press, Cambridge.

Chuvieco, E., L. Giglio, and C. Justice (2008), Global characterization of fire activity: Toward defining fire regimes from Earth observation data, *Global Change Biology*, *14*(7), 1488–1502.

Costa, L., K. Thonicke, B. Poulter, and F. Badeck (2011), Sensitivity of Portuguese forest fires to climatic, human, and landscape variables: Subnational differences between fire drivers in extreme fire years and decadal averages, *Regional Environmental Change*, *11*(3), 543–551.

Dee, D. P., *et al*. (2011), The ERA-Interim reanalysis: configuration and performance of the data assimilation system, *Quarterly Journal of the Royal Meteorological Society*, *137*(656), 553–597, doi:10.1002/qj.828.

De Wilde, L., and Chapin III, F. (2006), Human impact on the fire regime of interior Alaska: Interactions among fuels, ignition sources, and fire suppression, *Ecosystems*, *9*(8), 1342–1353, doi:10.1007/s10021-006-0095-0.

European Commission (2009), Forest Fires in Europe 2008, *JRC Scientific and Technical Report*, no. 9.

European Commission (2011), Forest Fires in Europe 2010, *JRC Scientific and Technical Report*, no. 11.

Flannigan, M. D., B. J. Stocks, and B. M. Wotton (2000), Climate change and forest fires, *Science of The Total Environment*, *262*(3), 221–229.

FCCC (2006), Report of the individual review of the greenhouse gas inventory of Portugal submitted in 2005, *Tech. rep*., FCCC/ARR/2005/PRT, http://unfccc.int/resource/docs/2006/arr/prt.pdf, Accessed 17 Feb 2010.

Giglio, L., J. T. Randerson, G. R. van der Werf, P. S. Kasibhatla, G. J. Collatz, D. C. Morton, and R. S. DeFries (2010), Assessing variability and long-term trends in burned area by merging multiple satellite fire products, *Biogeosciences*, *7*, 1171–1186, doi:10.5194/bg-7-1171-2010.

Guyette, R. P., R. M. Muzika, and D. C. Dey (2002), Dynamics of an anthropogenic fire regime, *Ecosystems*, *5*, 472–486, doi:10.1007/s10021-002-0115-7.

Heyerdahl, E. K., L. B. Brubaker, and J. K. Agee (2002), Annual and decadal climate forcing of historical fire regimes in the interior Pacific Northwest, USA, *Holocene*, *12*(5), 597–604.

Heyerdahl, E. K., P. Morgan, and J. P. Riser II (2008), Multi-season climate synchronized historical fires in dry forests (1650-1900), northern Rockies, USA, *Ecology*, *89*(3), 705–716.

Husari, S. J. and K. S. McKelvey (1996), Fire management policies and programs, in *Sierra Nevada Ecosystem Project: Final report to Congress, vol. II*, Chapt. 40, Davis: University of California, Centers for Water and Wildland Resources.

Janssen, P. H. M. and P. S. C. Heuberger (1995), Calibration of process-oriented models, *Ecological Modelling*, *83*(1–2), 55–56, doi:10.1016/0304-3800(95)00084-9.

Kaiser, J.W., A. Heil, M. O. Andreae, A. Benedetti, N. Chubarova, L. Jones, J.-J. Morcrette, M. G. Schultz, M. Suttie, and G. R. van der Werf (2012), Biomass burning emissions estimated with a global fire assimilation system based on observed fire radiative power, *Biogeosciences*, *9*(1), 527–554.

Keenan, T.F., et al. (2012), Terrestrial biosphere model performance for inter-annual variability of land-atmosphere CO 2 exchange, *Global Change Biology*, *18*(6), 1971–1987.

Kendall, M., and Stuart, A. (1983), The Advanced Theory of Statistics, Vol. 3, pp. 410–414, Griffin.

Klein Goldewijk, K. (2001), Estimating global land use change over the past 300 years: The HYDE database, *Global Biogeochemical Cycles*, *15*(4), 417–433.

Kloster, S., N. M. Mahowald, J. T. Randerson, and P. J. Lawrence (2012), The impacts of climate, land use, and demography on fires during the 21st century simulated by CLM-CN, *Biogeosciences Discussions*, *8*(5), 9709–9746.

Kloster, S., N. M. Mahowald, J. T. Randerson, P. E. Thornton, F. M. Hoffman, S. Levis, P. J. Lawrence, J. J. Feddema, K. W. Oleson and D. M. Lawrence (2010), Fire dynamics during the 20th century simulated by the Community Land Model, *Biogeosciences*, *7*(6), 1877–1902.

Krawchuk, M. A., and M. A. Moritz (2011), Constraints on global fire activity vary across a resource gradient, *Ecology*, *92*(1), 121–123.

Lawrence, D. M., K. W. Oleson, M. G. Flanner, P. E. Thornton, S. C. Swenson, P. J. Lawrence, X. Zeng, and A. G. Slater (2011), Parameterization improvements and functional and structural advances in Version 4 of the Community Land Model, *J. Adv. Model. Earth Syst.*, *3*(M03001), 1–27, doi:10.1029/2011MS000045.

Li, F., X. D. Zeng, and S. Levis (2012a), A process-based fire parameterization of intermediate complexity in a dynamic global vegetation model, *Biogeosciences*, *9*(7), 2761–2780.

Li, F., X. D. Zeng, and S. Levis (2012b), Quantifying the role of fire in the Earth system Part 1: Improved global fire modeling in the Community Earth System Model (CESM1), *Biogeosciences Discussions*, *9*, 1675316814, doi:10.5194/bgd-9-16753-2012.

Lindner, M., et al. (2010), Climate change impacts, adaptive capacity, and vulnerability of European forest ecosystems, *Forest Ecology and Management*, *259*(4), 698–709.

Lloret, F., E. Calvo, X. Pons, and R. Daz–Delgado (2002), Wildfires and landscape patterns in the Eastern Iberian Peninsula, *Landscape Ecology*, *17*(8), 745–759.

Loepfe, L., J. Martinez–Vilalta, J. Oliveres, J. Pinol, and F. Lloret (2010), Feedbacks between fuel reduction and landscape homogenisation determine fire regimes in three Mediterranean areas, *Forest Ecology and Management*, *259*(8), 2366–2374.

Loepfe, L., J. Martinez–Vilalta, and J. Pinol (2012), Management alternatives to offset climate change effects on Mediterranean fire regimes in NE Spain, *Climatic Change*, *115*(3–4), 693–707.

Mahecha, M. D., et al. (2010), Comparing observations and process-based simulations of biosphere-atmosphere exchanges on multiple timescales, *Journal of Geophysical Research G: Biogeosciences*, *115*(2), G02003.

Martell, E. K., L. B. Bevilacqua, and J. K. Stocks (1989), Modelling seasonal variation in daily people-caused fire occurrence, *Can. J. For. Res.*, *19*, 1555–1563, doi:10.1139/x89-237.

Meehl, G. A., et al. (2007), Global Climate Projections, in Climate Change 2007: The Physical Science Basis. Contribution of Working Group I to the Fourth Assessment Report of the Intergovernmental Panel on Climate Change, edited by S. Solomon, D. Qin, M. Manning, Z. Chen, M. Marquis, K.B. Averyt, M. Tignor, and H.L. Miller, Cambridge University Press, Cambridge, United Kingdom and New York, NY.

Murphy, P. B., D. J. Williamson, and D. M. J. S. Bowman (2011), Fire regimes: Moving from a fuzzy concept to geographic entity, *New Phytologist*, *192*(2), 316–318.

Mueller, B., and S. I. Seneviratne (2012), Hot days induced by precipitation deficits at the global scale, *Proceedings of the National Academy of Sciences*, *109*(31), 12398–12403, doi:10.1073/pnas.1204330109.

Pausas, J. G. (2004), Changes in fire and climate in the eastern Iberian Peninsula (Mediterranean Basin), *Climatic Change*, *63*(3), 337–350.

Pausas, J. G., J. Llovet, A. Rodrigo, and R. Vallejo (2008), Are wildfires a disaster in the Mediterranean basin? A review, *International Journal of Wildland Fire*, *17*(6), 713–723.

Pechony, O. and D. T. Shindell (2010), Driving forces of global wildfires over the past millennium and the forthcoming century, *Proceedings of the National Academy of Sciences*, *107*, 19167–19170, doi:10.1073/pnas.1003669107.

Pechony, O., and D. T. Shindell (2009), Fire parameterization on a global scale, *Journal of Geophysical Research D: Atmospheres*, *114*(16), D16115.

Prentice, I. C., D. I. Kelley, P. N. Foster, P. Friedlingstein, S. P. Harrison, and P. J. Bartlein (2010), Modeling fire and the terrestrial carbon balance, *Global Biogeochemical Cycles*, *25*(3), GB3005.

Pyne, S. J., P. L. Andrews, and R. D. Laven (1996), Introduction to Wildland Fire, 2nd Ed., Wiley Publishers, New York, NY.

Podour, J. J., and Martell, D. L. (2007), A simulation model of the growth and suppression of large forest fires in Ontario, *International Journal of Wildland Fire*, *16*, 285294.

Preisler, H. K., and Westerling, A. L. (2007), Statistical model for forecasting monthly large wildfire events in western United States, *Journal of Applied Meteorology and Climatology*, *46*, 1020–1030.

Rego, F. C., J. S. Silva, P. Fernandes, and E. Rigolot (2010), Solving the Fire Paradox â€“ Regulating the Wildfire Problem by the Wise Use of Fires, in Towards Integrated Fire Management - Outcomes of the European Project Fire Paradox, edited by J.S. Silva, F. C. Rego, P. Fernandes, and E. Rigolot, pp. 71–82, Springer-Verlag, Berlin.

R Development Core Team (2011), R Development Core Team, R Foundation for Statistical Computing, Vienna, Austria, Available for download from http://www.R-project.org.

Randerson, J. T., H. Liu, M. G. Flanner, S. D. Chambers, Y. Jin, P. G. Hess, G. Pfister, and C. S. Zender (2006), The impact of boreal forest fire on climate warming, *Science*, *314*(5802), 1130–1132, doi:10.1126/science.1132075.

Randerson, J. T., et al. (2009), Systematic assessment of terrestial biogeochemistry in coupled climate-carbon models, *Glob. Change Biol.*, *15* (10), 2462–2484, doi:10.1111/j.1365-2486.2009.01912.x.

San-Miguel-Ayanz, J., and Camia, A. (2009), Forest fires at a glance: facts, figures and trends in EU. European Forest Institute Discussion Paper 15, in Living with wildfires: what sciences can tell us, edited by Y. Birot, pp. 11–18, European Forest Institute, Finland.

San-Miguel-Ayanz, J., J. M. Moreno, and A. Camia (2013), Analysis of large fires in European Mediterranean landscapes: Lessons learned and perspectives, *Forest Ecology and Management*, Available online 5 January 2013, ISSN 0378-1127 doi: 10.1016/j.foreco.2012.10.050.

Schaefer, K., et al. (2012), A model-data comparison of gross primary productivity: Results from the north American carbon program site synthesis, *Journal of Geophysical Research G: Biogeosciences*, *117*(3), G03010.

Slocum, M. G., B. Beckage, W. J. Platt, S. L. Orzell, and W. Taylor (2010), Effect of Climate on Wildre Size: A Cross-Scale Analysis, *Ecosystems*, *13*(6), 828–840.

Simmons, A. J., K. M. Willett, P. D. Jones, P. W. Thorne, and D. P. Dee (2010), Low-frequency variations in surface atmospheric humidity, temperature, and precipitation: Inferences from reanalyses and monthly gridded observational data sets, *J. Geophys. Res.*, *115*, D01110, doi:10.1029/2009JD012442.

Stöckli, R., D. M. Lawrence, G. -Y. Niu, K. W. Oleson, P. E. Thornton, Z.-L. Yang, G. B. Bonan, A. S. Denning, and S. W. Running (2008), The use of Fluxnet in the Community Land Model development, *J. Geophys. Res.*, *113*, G01025, doi:10.1029/2007JG000562.

Stocks, B. J., et al. (2003), Large forest fires in Canada 1959-1997, *Journal of Geophysical Research*, *108*, D18149, doi:10.1029/2001JD000484.

Swetnam, T. W., and J. Betancourt (1998), Mesoscale disturbance and ecological response to decadal climate variability in the American Southwest, Journal of Climate, II, 3128–3147.

Theobald, D. M., and W. H. Romme (2007), Expansion of the US wildland-urban interface, *Landscape and Urban Planning*, *83*(4), 340–354.

Thonicke, K., S. Venevsky, S. Sitch, and W. Cramer (2001), The role of fire disturbance for global vegetation dynamics: Coupling fire into a dynamic global vegetation model, *Global Ecology and Biogeography*, *10*(6), 661–677.

Thonicke, K., A. Spessa, I. C. Prentice, S. P. Harrison, L. Dong, and C. Carmona–Moreno (2010), The influence of vegetation, fire spread and fire behaviour on biomass burning and trace gas emissions: Results from a process-based model, *Biogeosciences*, *7*(6), 1991–2011.

Thornton, P. E., J. F. Lamarque, N. A. Rosenbloom, and N. M. Mahowald (2007), Influence of carbonnitrogen cycle coupling on land model response to CO2 fertilization and climate variability, *Global Biogeochemical Cycles*, *21*, GB4018, doi:1029/2006GB002868.

Thornton, P. E., S. C. Doney, K. Lindsay, J. K. Moore, N. M. Mahowald, J. T. Randerson, I. Fung, J. F. Lamarque, J. F. Feddema, and Y. -H. Lee (2009), Carbon-nitrogen interactions regulate climate-carbon cycle feedbacks: Results from an atmosphere-ocean general circulation model, *Biogeosciences*, *6*(10), 2099–2120, doi:10.5194/bg-6-2099-2009.

van der Werf, G. R., J. T. Randerson, L. Giglio, N. Gobron, and A. J. Dolman (2008), Climate controls on the variability of fires in the tropics and subtropics, *Global Biogeochemical Cycles*, *22*, GB3028, doi:10.1029/2007GB003122.

van der Werf, G. R., L. Giglio, J. T. Randerson, G. J. Collatz, G. J. Mu, P. S. Kasibhatla, D. C. Morton, R. S. DeFries, Y. Jin, and T. T. van Leeuwen (2010), Global fire emissions and the contribution of deforestation, savanna, forest, agricultural, and peat fires (1997 – 2009), *Atmos. Chem. Phys.*, *10*, 11707–11735, doi:10.5194/acp-10-11707-2010.

Venevsky, S., K. Thonicke, S. Sitch, and W. Cramer (2002), Simulating fire regimes in human-dominated ecosystems: Iberian Peninsula case study, *Global Change Biology*, *8*(10), 984–998.